

# **Physical Confinement during Cancer Cell Migration Triggers Therapeutic Resistance and Cancer Stem Cell-like Behavior**

Qionghua Shen<sup>1</sup>, Tamara Hill<sup>1</sup>, Xue Cai<sup>2</sup>, Loan Bui<sup>3</sup>, Rami Barakat<sup>1</sup>, Emily Hills<sup>1</sup>, Turki Almugaiteeb<sup>4</sup>, Anish Babu<sup>5</sup>, Patrick H Mckernan<sup>5</sup>, Michelle Zalles<sup>6</sup>, James D Battiste<sup>5\*</sup> and Young-Tae Kim<sup>1,7\*</sup>

<sup>1</sup>*Neuroengineering Lab, Department of Bioengineering, University of Texas at Arlington, TX*

<sup>2</sup>*Department of Neurosurgery, University of Oklahoma Health Sciences Center, OK*

<sup>3</sup>*Department of Aerospace & Mechanical Engineering, University of Notre Dame, IN*

<sup>4</sup>*RPD Innovations, Riyadh, Saudi Arabia*

<sup>5</sup>*Department of Neurology, University of Oklahoma Health Sciences Center, OK*

<sup>6</sup>*Oklahoma Medical Research Foundation, OK*

<sup>7</sup>*Department of Urology, UT Southwestern Medical Center, TX*

## **Supplementary Information**

## Supplementary Methods

### Microchannel Device Design

An engineered combination of PDMS devices were collected and applied to our study. PDMS devices were fabricated by negative photolithography combined with soft lithography. The flower device contains  $5\mu\text{m} \times 5\mu\text{m}$  microchannels. Six independent reservoirs can separate and collect cells that migrated through physical confinements (Fig. S1. A). Satellite reservoirs were individually connected to a central reservoir to guarantee the purity for each cell group but control the cells under the same testing condition. The long device contains 600 microchannels with a dimension of  $5\mu\text{m} \times 12\mu\text{m}$  (length  $\times$  width). The total length of a single microchannel is around 5mm which could hold enough cells inside for protein collection (Fig. S1. B). Cells outside microchannel were considered as 2D cultured cells; cells migrating inside microchannel were considered as migrating cells and collected for Western blot analysis; cells that crept throughout the microchannel were considered to be migrated cells and used for drug studies and immunostaining (Fig. S1. C). Fig. S1. D demonstrates the protein collecting process.

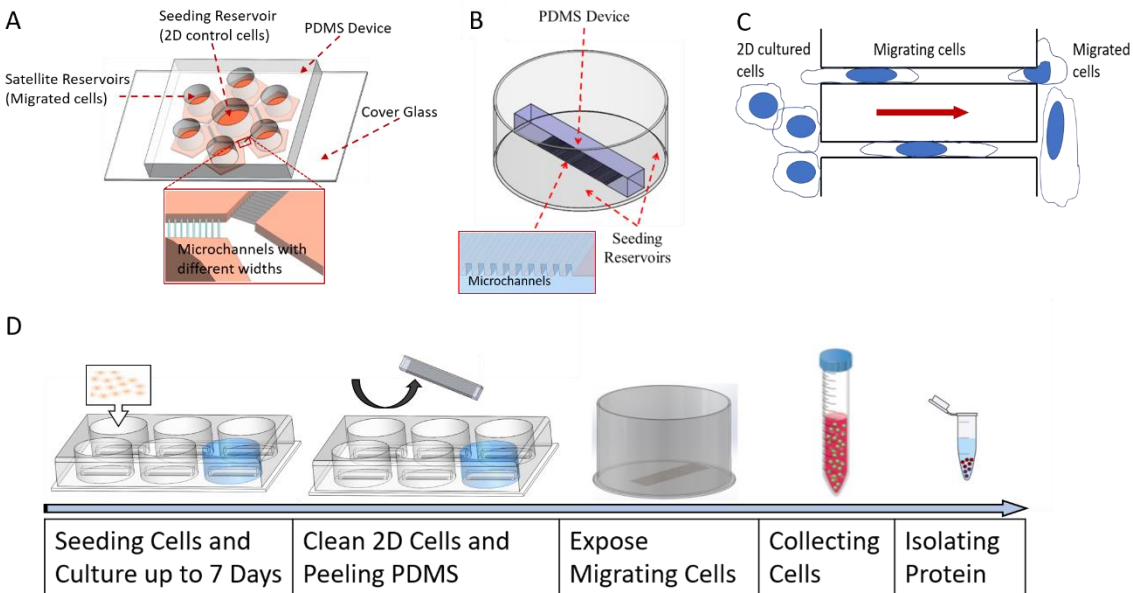


**Figure S1.** **A.** A flower device equipped with different dimensioned microchannels for drug testing and immunostaining. **B.** A long device equipped with extensive microchannels for migrating cells collection. **C.** Demonstrational image of 2D cultured cells, migrating cells and migrated cells (Red arrow indicated cell migrating direction). **D.** Procedures for migrating cell and protein collection.

### **ABCG2 Inhibition Test**

Three groups of flower devices with enough migrating G55 cells were treated with 17 $\mu$ M Dox, 5 $\mu$ M Fumitremorgin C (FTC), or 17 $\mu$ M Dox + 5 $\mu$ M FTC for 4 hours at 37°C. Autofluorescence images were taken for Dox, FTC and Dox + FTC groups after the addition of a fresh image medium. Samples were kept in the image medium overnight, and then were stained with the Live/Dead staining for 10 minutes at room temperature. Again, respective images were obtained. Dox autofluorescence was quantified by ImageJ and the cell viability was calculated based on the Live/Dead staining signals.

### **Quantification of Collected Migrating Cells**

Hoechst33342 (Invitrogen) staining of the nuclei was used to count total cell numbers. G55 cells were cultured in the long devices (n=3) for 5 days to initiate migrating cells. After 2D cells were removed by Trypsin-EDTA, devices were stained with Hoechst33342 for 1 hour and FDA-PI (for live and dead cell counting, respectively) for 20 minutes at 37°C. PDMS microchannel devices were peeled to expose the migrating cells. Hoechst33342 signals of the entire microchannel device were recorded by video. Fluorescent images for Hoechst/FDA/PI signals were taken at 3 randomly picked sites from each device under 20 x objectives (Fig. S3. B).

### **Hypoxia Culture**

A custom-built hypoxia chamber constructed from a polycarbonate, air-tight container. A mixture of 90% nitrogen, 5% carbon dioxide and 5% oxygen was used to purge the hypoxia chamber. Cells were cultured in hypoxic condition (< 5% oxygen) for 72 hours, and the chamber was purged once a day at 24-hour intervals.

### **Total Protein Quantification**

Total protein samples with equal amount (24  $\mu$ l) were loaded into two pieces of 10% SDS-page gels for all Western blot tests samples. One gel was electro-transferred to a PVDF membrane for further Western blot study. The other was stained by the Brilliant Blue to visualize total protein bands. Quantification of the intensities of the bands was performed by ImageJ. The transferred PVDF membrane was detected by GAPDH antibody (1:5,000, HRP-60004, Proteintech) to indicate the protein loading amount.

## **Results and Discussion**

### **FTC ABCG2 Inhibition**

FTC is a well-established and widely used ABCG2 inhibitor. In this study, the changes of Dox intensities were shown as overnight intensity minus 4 hour intensity. The FTC alone data were not shown in Fig. S2. A (due to the absence of auto-fluorescence of the FTC), but we did use it as a background control for signal quantification in Dox + FTC group. In the G55 2D group, nuclear Dox intensities were slightly increased in Dox (about 4 units) and Dox + FTC (about 6 units) groups. In the 5x5  $\mu$ m microchannel groups, an overnight intensity decrease was significantly bigger in Dox groups than in Dox + FTC groups, in which the intensity dropped in Dox groups was 27 units and the intensity dropped in Dox + FTC groups was 3.4 units, indicating an obvious DOX pumping out inhibition by FTC (Fig. S2. A). Our results suggest that during robust migration via tightly confined spaces the cells acquire more ABCG2 proteins in the cell membrane so that the migrating cancer cells can pump out the DOX molecules via efflux proteins which are significantly inhibited by FTC, ABCG2 inhibitor. Correspondingly, in microchannel groups, overnight cell viability in Dox + FTC treated groups was about 20% low as compared to Dox treated ones. No significant eradicating effect was observed in only FTC treated groups (Fig. S2. B).

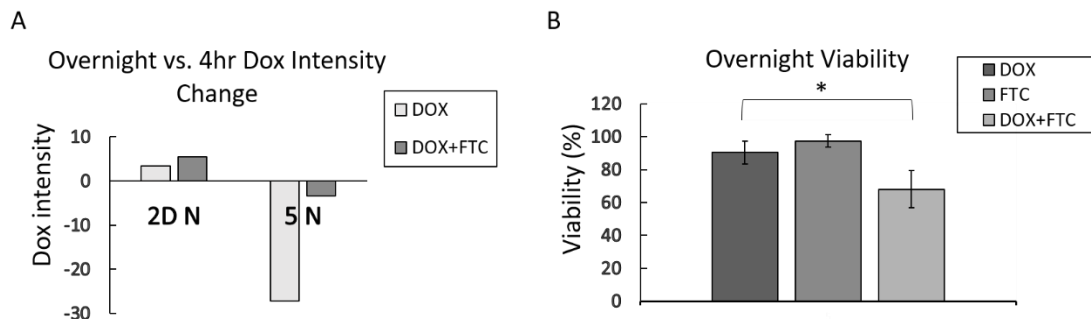


**Figure S2. A.** Dox intensity changes between at 4 hours and after overnight incubation. Data are presented as overnight DOX intensities minus 4 hours DOX intensities (2D N: nucleus DOX intensity in central area; and 5 N: nucleus DOX intensity in cells migrated through 5x5  $\mu\text{m}$  microchannels).  $N \geq 25$  cells/condition. **B.** Overnight viability of cells in three different conditions (DOX, FTC, or DOX + FTC) migrated through 5x5  $\mu\text{m}$  microchannels. Cell viability was analyzed by a Live/Dead Stain.  $N \geq 65$  cells/condition. \* $p < 0.05$  between DOX and DOX + FTC.

### Quantification of Collected Migrating Cells

About  $3356 \pm 68$  migrating G55 cells were collected from each long device with our collecting method. This equated to almost  $6 \times 10^4$  cells that were collected from 18 devices totally for protein analysis study (Fig. S3. A, Left) with an almost 94% cell viability (Fig. S3. A, Right). Representative fluorescent images showed consistent results of the viability (Fig. S3. B).

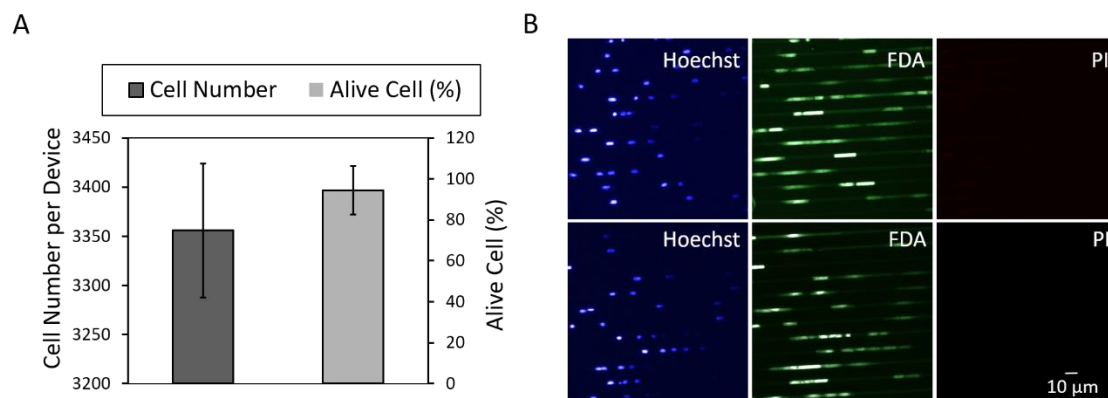


**Figure S3. A.** G55 cell number (left) and cell viability [1] from each long device after peeling. Cell viability was calculated by Hoechst33342 and PI staining. **B.** Two representative images of migrating G55 cells inside the long device (top and bottom). Blue: Hoechst33342 (total cells); Green: FDA (live cells); and Red: PI (dead cells).

### Comparison of Hypoxia Induced Factor expression between Hypoxia and confined-migrating cancer cells under normoxia

Two times elevated HIF-1 $\alpha$  expression was observed in the migrating G55 under normoxia as compared to in the G55 under hypoxia (Fig. S4). This result suggests that the robustly migrating cancer cells can produce significantly higher amount of the HIF-1 $\alpha$  under normoxia condition than the same cancer cells cultured under hypoxia condition.

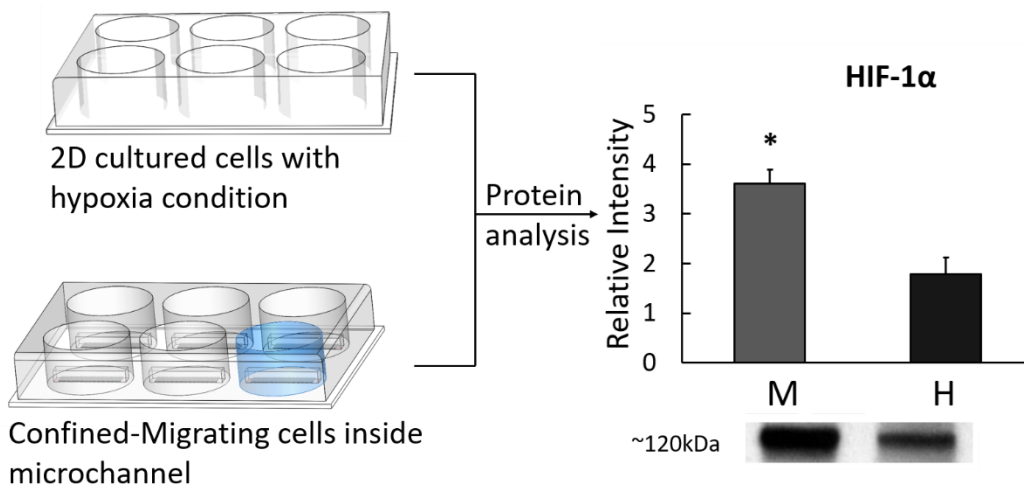


**Figure S4.** Two times elevated HIF-1 $\alpha$  expression in the confined-migrating group as compared to hypoxic chamber group. G55 western blot results are shown as Average + Std. Representative blot images of each marker are shown below their respective graphs. M = migrating G55 cells under normoxia (e.g., 20% oxygen) and H = G55 cells under hypoxia (e.g., < 5% oxygen). All results were normalized to the total proteins. \*p<0.05. All experiments were reproduced.

### Total Protein Quantification

For both cell lines (G55 and MDA-MB-231), although we attempted to load equal amount of proteins based on the protein concentration, the gel staining showed inequality (Fig. S5. A and C). GAPDH bands turned to be inconsistent with total gel staining. It has been pointed out that

GAPDH or  $\beta$ -actin (i.e., well-established Western blot loading controls) signal could be affected by hypoxia and/or migration for certain cancer types. Alternatively, that total protein stain is believed with much less variable across samples and has a grater linear range than GAPDH and  $\beta$ -actin [2, 3]. Moreover, it has been reported that Coomassie staining has low cost, high reliability and compatibility [4]. Therefore, we decided to utilize the results of total proteins from gel staining for normalization and for accurate quantification.

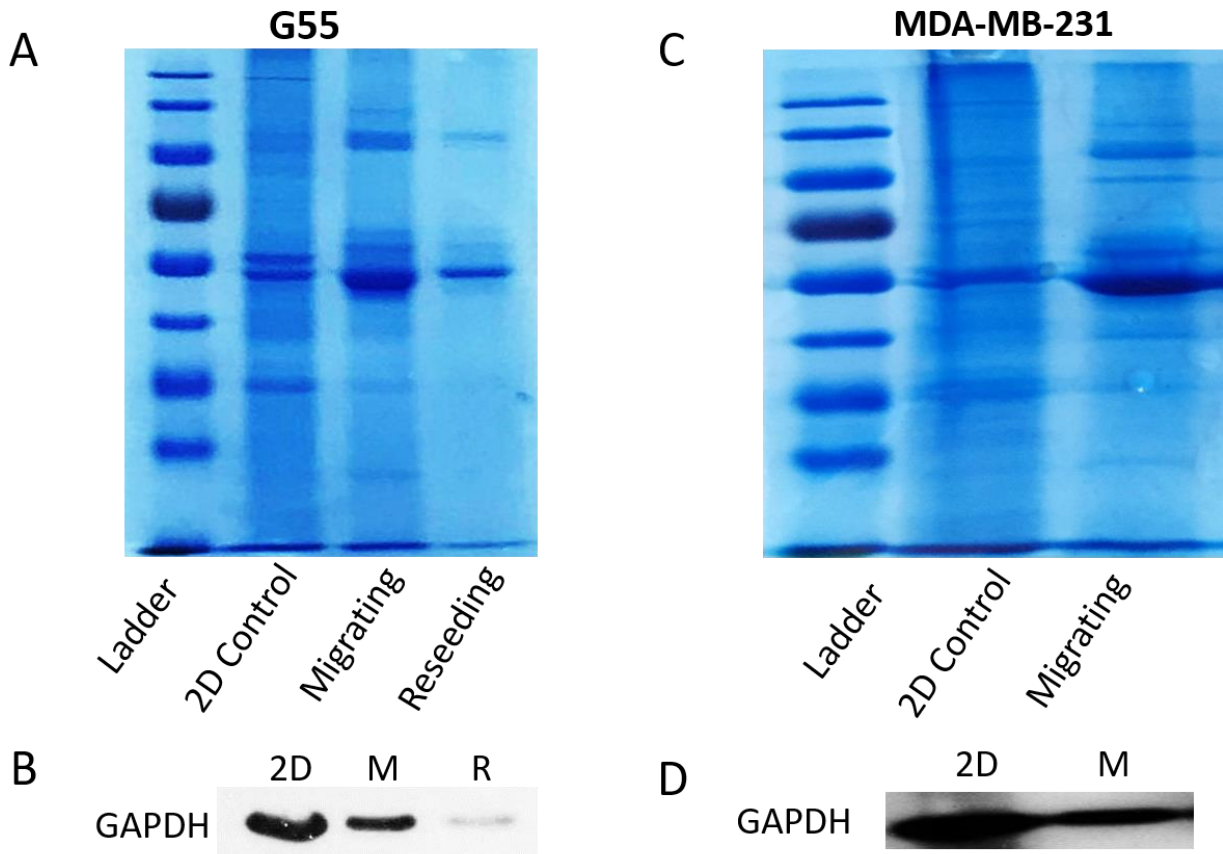


**Figure S5.** Gel staining for total proteins and Western blot for detecting GAPDH. G55 (A) and MDA-MB-231 (C) gels with Brilliant Blue staining for total protein analysis, and corresponding Western blots of GAPDH (B and D). (2D: Non-migrating cells; M: migrating cells; and R: reseeded migrating cells).

### Immunohistochemical Staining for CD133 in the G55 Murine Xenograft Model

A high percentage of CD133 positive G55 cells were detected when tumor cells migrated to physically confined areas (e.g. parenchyma and whiter matter tracts). Higher expression of CD133 could be detected from distant metastatic G55 via white matter.

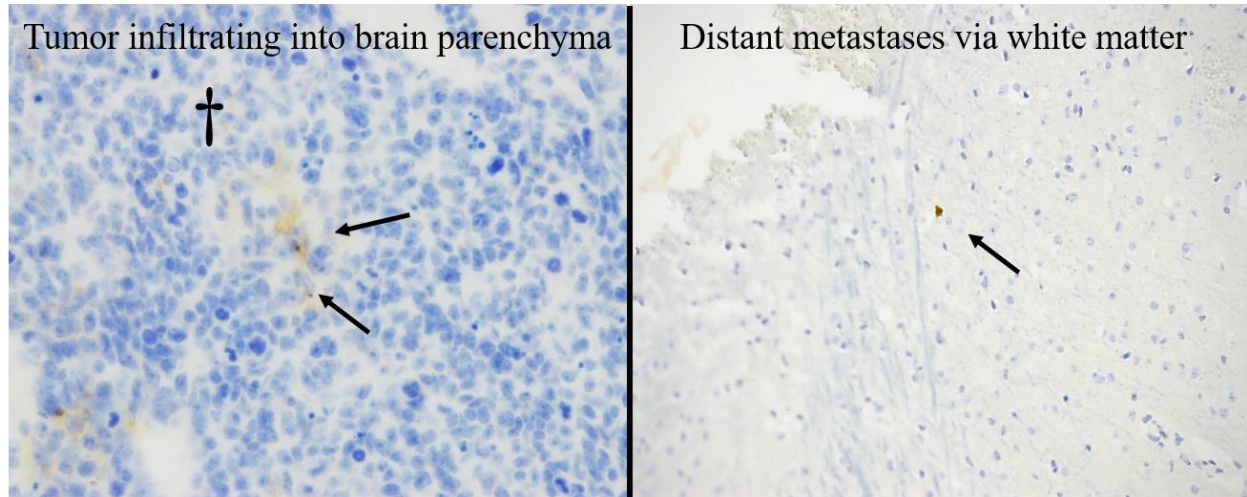


**Figure S6.** Immunohistochemical staining for CD133 in the G55 murine xenograft model with DAB secondary. PDX mouse model with G55 tumor cells implanted into the striatum of a mouse by stereotactic injection. Antibody hybridization with the anti-CD133 antibody. The left representative image showed CD133 positive G55 cells in the physically confined brain parenchyma area. The right side image demonstrated high CD133 expression for migrated G55 within white matter tracts. Arrow: CD133 positive G55 cells. †: Border of G55 tumor.

#### Reference:

- [1] M.H. Wright, A.M. Calcagno, C.D. Salcido, M.D. Carlson, S.V. Ambudkar, L. Varticovski, Brca1 breast tumors contain distinct CD44(+)/CD24(-) and CD133(+) cells with cancer stem cell characteristics, *Breast Cancer Research*, 10 (2008).
- [2] J.S. Thacker, D.H. Yeung, W.R. Staines, J.G. Mielke, Total protein or high-abundance protein: Which offers the best loading control for Western blotting?, *Analytical biochemistry*, 496 (2016) 76-78.
- [3] S.L. Eaton, S.L. Roche, M.L. Hurtado, K.J. Oldknow, C. Farquharson, T.H. Gillingwater, T.M. Wishart, Total protein analysis as a reliable loading control for quantitative fluorescent Western blotting, *PloS one*, 8 (2013) e72457.
- [4] C. Welinder, L. Ekblad, Coomassie staining as loading control in Western blot analysis, *Journal of proteome research*, 10 (2011) 1416-1419.